Dependence of Alkyl Chain Conformation of Simple Ionic Surfactants on Head Group Functionality As Studied by Vibrational Sum-Frequency Spectroscopy

John C. Conboy,† Marie C. Messmer,‡ and Geraldine L. Richmond*

Department of Chemistry, University of Oregon, Eugene, Oregon 97403

Received: June 6, 1997[⊗]

The conformational order of sodium dodecyl sulfate (SDS), sodium dodecylsulfonate (DDS), dodecyltrimethylammonium chloride (DTAC), and dodecylammonium chloride (DAC) adsorbed at the D_2O/CCl_4 interface has been examined by total internal reflection sum-frequency vibrational spectroscopy (VSFS). The vibrational sum-frequency spectra indicate the presence of gauche conformations in the hydrocarbon chains of SDS, DDS, DTAC, and DAC at all surface coverages examined. An increase in the surface concentration of surfactant at the D_2O/CCl_4 interface results in the reduction of gauche defects in the hydrocarbon chain as determined from the intensity ratio of the methyl to methylene symmetric stretch vibrational modes. Analysis of the SF vibrational spectra suggest significantly different alkyl chain conformations for the cationic and anionic surfactants examined. The alkyl chains of the cationic surfactants DTAC and DAC possess the fewest gauche defects, while SDS and DDS display more disorder in the hydrocarbon chains at similar surface concentrations. Mixed surfactant monolayers are also examined and are observed to display the least number of gauche defects, attributed to a reduction in head group repulsion.

I. Introduction

Whereas much has been learned in recent years on a molecular level about how amphiphillic molecules adsorb at air/liquid interfaces, much less is known about their behavior at the oil/water interface. This is particularly true for simple water soluble surfactants that are commonly used in commercial products.[1−3] This lack of information is primarily due to the absence of experimental methods for studying the liquid/liquid interface on a molecular level. While studies have been done to determine the orientation and adsorption properties of surface active dyes at the oil/water interface using fluorescence,[4,5] resonance Raman scattering,[6−8] and second harmonic generation (SHG),[9−11] little is known about the alkyl chain conformation of simple alkyl surfactants at the liquid/liquid interface and how such factors as head group functionality and surface concentration play a role in conformational order. Most neutron reflection and X-ray diffraction studies of surfactants have been conducted at the air/water interface.[12−16] Such techniques have only recently been applied to the investigation of surfactants at the liquid/liquid interface.[17,18]

Vibrational sum-frequency spectroscopy (VSFS) has been used in this work to measure the vibrational spectra of a number of simple water soluble ionic surfactants adsorbed at the D_2O/CCl_4 interface. An understanding of these systems in relevant in advances in enhanced oil recovery as well as the technologically important field of emulsions.[2,19] The surfactant molecules that reside at the interface have their hydrophobic alkyl tails in the oil phase and the hydrophilic cationic or anionic head group in the water phase. In previous studies of these types of surfactants at air/water interfaces, where the alkyl tails assemble in the vapor above the liquid phase, much has been learned about how surface density affects molecular structure.[2,3,20,21] The van der Waals interactions between the alkyl chains of surfactants play a very important role in how the surfactants assemble at the air/water interface. These attractive forces can counter the repulsive electrostatic forces between the charged surfactant head groups, leading to a relatively ordered assembly of surfactant molecules. At the liquid/liquid interface, the van der Waals attractions between alkyl surfactants can be diminished as solvent diffuses between the chains. Under such conditions the chemical and electrostatic environment of the hydrophilic head group plays an even greater role in the adsorption behavior of the surfactants.[22] The goal of these studies is to determine if the chemical nature of the ionic head group affects the packing density and subsequent alkyl chain disorder by way of either electrostatic repulsion or size (possibly including the solvation sphere).

In this paper, the conformational order of sodium dodecyl sulfate (SDS), sodium dodecylsulfonate (DDS), dodecyltrimethylammonium chloride (DTAC), and dodecylammonium chloride (DAC) adsorbed at the D_2O/CCl_4 interface are examined in detail by VSFS. With VSFS, the molecular structure sensitivity of vibrational spectroscopy is coupled with the interface specificity of this nonlinear technique to make it an ideal probe for examining buried interfaces.[23−34] A total internal reflection geometry is used, which significantly enhances the sensitivity of this technique, allowing measurements to be made over a wide range of surface concentrations. The sum-frequency vibrational spectra of SDS, DDS, DTAC, and DAC are examined, first, to characterize the vibrational modes being probed and, second, to understand the effect of increased surface concentration on the ordering of the alkyl chains. Information about molecular conformation of the hydrocarbon chain is obtained specifically from the C−H symmetric stretch region of the vibrational spectra. Conformational order is discussed in terms of the surface concentration of surfactant and the character of the ionic head group.

II. Background

Sum-Frequency Vibrational Spectroscopy. Sum-frequency vibrational spectroscopy has one major advantage over conventional linear vibrational surface spectroscopic methods in that it is inherently interface specific. In IR−vis sum-frequency generation SFG, two coherent laser beams, one visible and the

† Present address: Department of Chemistry, University of Minnesota, 207 Pleasant St., Minneapolis, MN 55455.

‡ Present address: Department of Chemistry, Lehigh University, 6 East Packer Avenue, Bethlehem, PA 18015-3172.

⊗ Abstract published in *Advance ACS Abstracts,* August 1, 1997.

S1089-5647(97)01867-1 CCC: $14.00

other from a tunable IR laser source (ω_1 and ω_2) impinge on a surface. The induced nonlinear polarization results in the coherent generation of light at the sum-frequency ($\omega_3 = \omega_1 + \omega_2$), the intensity of which is governed by the surface polarization.[35] The sum-frequency intensity is given by following expression

$$I(\omega_{SF}) = |\tilde{f}_{SF} P^{(2\omega)}(\omega_{SF})|^2 \quad (1)$$

where $P^{(2\omega)}$ is the induced second-order polarization and $\tilde{f}_{SF}$ is the nonlinear Fresnel factor for the generated sum-frequency light.[36,37] The induced nonlinear polarization in a medium is given by

$$P^{(2)}(\omega_{SF}) = \chi^{(2)} : \hat{e}_{\omega_1} \hat{e}_{\omega_2} \sqrt{I_{\omega_1}} \sqrt{I_{\omega_2}} \quad (2)$$

where I is the laser intensity for each of the input beams ω_1 and ω_2 and $\chi^{(2)}$ is the second-order susceptibility tensor. In the expression above, $\hat{e}_i = \hat{\epsilon}_i f_i$, where $\hat{\epsilon}_i$ is the unit polarization vector and f_i is the geometric Fresnel factor. The symmetry constraints on $\chi^{(2)}$ prohibit nonlinear interactions in the bulk of centrosymmetric medium. At an interface, this constraint is lifted and such processes are allowed due to the local break in symmetry. As a result, the spectroscopy of the molecules residing in the interfacial region can be probed selectively without any contributions from the molecules present in the more pervasive bulk liquids.

The second-order susceptibility $\chi^{(2)}$ can be separated into a nonresonant contribution $\chi^{(2)}_{NR}$ arising from the bare interface and a resonant contribution $\chi^{(2)}_{R}$ arising from the vibrational resonances of the molecules at the interface:

$$\chi^{(2)} = \chi^{(2)}_{NR} + \sum_{\nu} \chi^{(2)}_{R}(\nu) \quad (3)$$

Because the elements of $\chi^{(2)}_{NR}$ and $\chi^{(2)}_{R}$ and the associated Fresnel factors may be complex, interference between terms can exist. For this reason the relative phase of the terms in eq 3 must be taken into account. For the studies presented here, within the C−H stretch spectral region the nonresonant component from the D_2O/CCl_4 interface has been found to be minimal with the SF response being dominated by the resonant susceptibility of vibrational modes in the introduced surfactant. For an IR vibrational mode, the resonant component of the susceptibility is given by[35,38]

$$(\chi^{(2)}_{R}(\omega_{IR}))_{lmn} = \sum_{\nu} \frac{N A_{n_\nu} M_{lm_\nu} \Delta p}{(\omega_\nu - \omega_{IR} - i\Gamma_\nu)} \quad (4)$$

where N is the adsorbate surface density, $A_{n\nu}$ is the IR transition moment, M_{lm_ν} is the Raman transition moment, Δp is the population difference, ω_ν is the transition frequency with a damping constant of Γ_ν for a specific transition, ν, and ω_{IR} is the frequency of the incident infrared beam. In order for a transition to be SFG active, it must satisfy the constraint of eq 4, which requires that the vibrational transition be both infrared and Raman allowed.

With a judicious choice of both the input and output polarizations, the independent tensor elements of $\chi^{(2)}_{R}$ can effectively be isolated. There are four such polarization combinations that are of interest when probing the liquid/liquid interface with SFG. The expressions for the SF intensity for the relevant polarization combinations are given by the following

$$I^{sum}_{ssp} \propto |\tilde{f}_y E_1(\omega_1)\, E_2(\omega_2) \sin\theta_2\, f_{1y} f_{2z} \chi_{iiz}|^2 \quad (5a)$$

$$I^{sum}_{sps} \propto |\tilde{f}_y E_1(\omega_1)\, E_2(\omega_2) \sin\theta_1\, f_{1z} f_{2y} \chi_{izi}|^2 \quad (5b)$$

$$I^{sum}_{pss} \propto |\tilde{f}_z E_1(\omega_1)\, E_2(\omega_2) f_{1y} f_{2y} l \chi_{zii}|^2 \quad (5c)$$

$$\begin{aligned} I^{sum}_{ppp} \propto |&\tilde{f}_x E_1(\omega_1)\, E_2(\omega_2)(\cos\theta_1 \sin\theta_2\, f_{1x} f_{2z} \chi_{iiz} + \\ &\sin\theta_1 \cos\theta_2\, f_{1z} f_{2x} \chi_{izi}) + \\ &\tilde{f}_z E_1(\omega_1)\, E_2(\omega_2) \cos\theta_1 \cos\theta_2\, f_{1x} f_{2x} \chi_{zii} + \\ &\tilde{f}_z E_1(\omega_1)\, E_2(\omega_2) \sin\theta_1 \sin\theta_2\, f_{1z} f_{2z} \chi_{zzz}|^2 \end{aligned} \quad (5d)$$

where the first letter of the intensity subscript refers to the polarization of the output sum-frequency, the second for the visible, and the third for the IR source, θ_1 and θ_2 are the incident angles of the visible and IR light, f's are the linear Fresnel factors discussed above, and E is the electric field strength. By selecting the appropriate polarizations, one can effectively isolate the SF response as a function of the IR polarization. This can be used to determine the net dipole polarization of a vibrational transition parallel or perpendicular to the surface normal.[30,39−41] Such measurements allow for the determination of the conformational and orientation of molecular species residing at the interface as will be illustrated in the following sections.

In addition to a strong resonant contribution from the C−H stretching vibrations within the molecules, the intensity is also dependent upon the Fresnel factors for the input fields, f_i, and the outgoing SF, $\tilde{f}_{SF}$, as shown in eqs 1 and 2. In this way, the detected SF signal is dependent upon the optical properties of the two bulk media through their frequency-dependent refractive indices and the optical geometry, internal vs external. In the case of linear spectroscopic methods such as FTIR attenuated total reflection (ATR), this dependence has been used to enhance the sensitivity of these methods.[42−44] In a similar fashion, total internal reflection sum-frequency generation (TIR SFG) is used here to measure the sum-frequency vibrational spectrum of surfactants adsorbed at a liquid/liquid interface. An enhancement of several orders of magnitude in the SF response is calculated for an internal reflection geometry above that of an external reflection geometry.[26,28,36,37,45−47] For the case of internal reflection, the linear and nonlinear Fresnel factors in eqs 1 and 2 take on imaginary values at incident angles above the critical angles for the incident visible and IR fields. The local field intensity at the interface exceeds that found in an external reflection geometry due to the formation of an evanescent wave at the interface. The maximum in the SF intensity occurs when the fundamental beams approach the interface at their respective critical angles. It is this implementation of a TIR optical geometry that has allowed the investigation of this fluid interface, which has previously been inaccessible by conventional SFG.

III. Experimental Section

Materials. D_2O (99%) and HPLC grade CCl_4 were purchased from Aldrich. The CCl_4 was distilled in order to remove any residual hydrocarbon compounds, and its purity was confirmed by transmission FTIR. D_2O was shaken with purified CCl_4 prior to use and decanted. Sodium dodecyl sulfate (SDS) (Aldrich, 99.8%), sodium dodecylsulfonate (DDS) (TCI America, 99%), dodecyltrimethylammonium chloride (DTAC) (TCI America, 99%), and dodecylammonium chloride (DAC) (Kodak, 98%) were used as received. Hexadecyl sulfate (SHDS) was prepared by sulfonation of 1-hexadecanol (99% Aldrich) with

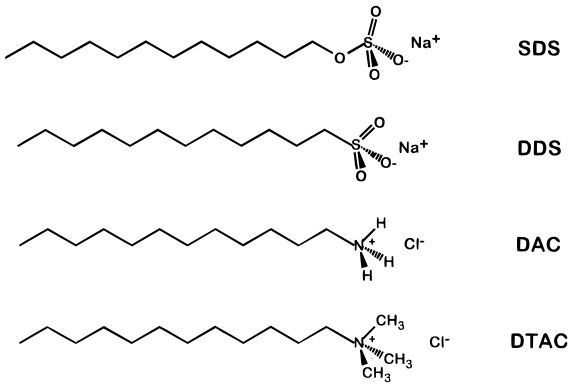

Figure 1. Molecular structures of sodium dodecyl sulfate (SDS), sodium dodecylsulfonate (DDS), dodecyltrimethylammonium chloride (DTAC), and, dodecylammonium chloride (DAC).

chlorosulfonic acid (99% Aldrich).[48] Sodium hexadecyl-d_3 sulfate was prepared by $LiAlH_4$ reduction in tetrahydrofuran of palmitic-d_3 acid. The hexadecane-d_3 sulfate was then obtained by sulfonation of the resulting alcohol with chlorosulfonic acid. Purity of the products was determined by FTIR and NMR. The molecular structures for the surfactants used, SDS, DDS, DTAC, and DAC, are shown in Figure 1.

Sum-Frequency Experiments. Tunable IR light was generated using a $LiNbO_3$ optical parametric oscillator (OPO), described elsewhere.[49] The OPO was pumped with the fundamental output of a Q-switched Nd:YAG laser generating 1064 nm pulses at 10 Hz with a pulse duration of 12 ns. Tunability throughout the desired wavelength region was achieved by angle tuning the $LiNBO_3$ crystal. IR light pulses in the 2700−3100 cm^{-1} region with a band width of 6 cm^{-1} and energies of 2−3 mJ were obtained over the entire spectral region. Calibration of the OPO was performed using a polystyrene sample. The remainder of the 1064 nm YAG fundamental was frequency doubled in a KDP crystal to generate the visible 532 nm light.

The sum-frequency experiments were performed in a cylindrical quartz cell. In order to achieve the desired optical geometry for total internal reflection, both the visible and IR beams were directed onto the D_2O/CCl_4 interface through the CCl_4, high index phase, in a copropagating manner. D_2O was used instead of H_2O due to the weak but significant absorption by H_2O in the spectral region of interest, which resulted in notable heating of the interface. The IR was focused on the interface at an angle of 70°. The visible 532 nm was collimated to a diameter of 1−2 mm and incident on the interface at an angle of 66°. Laser powers used were typically 1−2 mJ/pulse between 2800 and 3100 cm^{-1} and 5 mJ/pulse at 532 nm.

The sum-frequency signal was collected in reflection at an angle of 66°. The resulting sum-frequency light was polarization selected with a broad band Glann-Taylor polarizer. The residual 532 nm light was removed by a combination of absorptive, interference, and holographic notch filters. The resulting signal was detected using a PMT and gated electronics. Variation of the input IR polarization was accomplished with a Soleil-Babinet compensator and an IR polarizer. Polarization of the visible light was selected with a half-wave plate. Data points, collected every 2 cm^{-1}, were an average of 200 pulses. The SF spectra were corrected for Fresnel contributions for each polarization and for the intensity variation of the infrared beam throughout the spectral region.

The sample cell used in the SF experiments was cleaned with MicroCleaner and Nochromix solution and rinsed with NANOpure water that had a resistivity of 17.9 MΩ cm. The cell was dried in an oven at 100 °C to remove residual water. The solvents CCl_4 and D_2O were introduced into the sample cell and allowed to equilibrate. No detectable SF signal resulted from the bare D_2O/CCl_4 interface. This measurement also served as a means of determining the presence of any surface active contaminants. The surfactants SDS, DDS, DTAC, and DAC were added to the cell by removing an aliquot of the D_2O and dissolving the desired amount of surfactant. The solution was then returned to the cell and mechanically stirred. SF spectra were collected after allowing the solutions to equilibrate for 20 min. A pH of 4.5−5.0 was measured for the D_2O solutions used. No adjustment to the pH was made for any of the solutions. All spectra were obtained at room temperature.

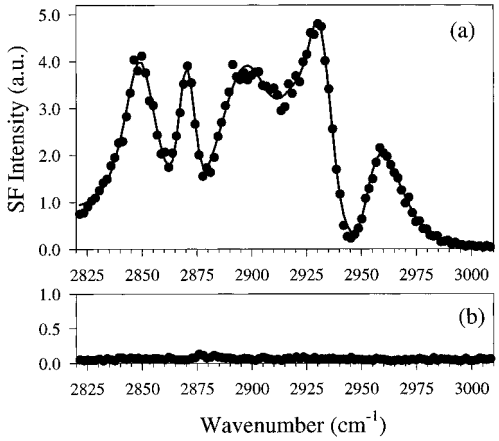

Figure 2. Sum-frequency vibrational spectrum of (a) 5.0 mM SDS at the D_2O/CCl_4 interface and (b) the bare D_2O/CCl_4 interface. The polarizations used were p for visible, p for infrared. The sum-frequency output light was collected with no polarization selection. The solid lines represent a fit to the spectra using a combination of Gaussian and Lorentzian functions for each peak.

Interfacial Tension Measurements. Interfacial tension measurements of SDS, DDS, DTAC, and DAC at the H_2O/CCl_4 interface were obtained by means of the drop-volume method.[50] A Gilmont micrometer syringe was used for drop delivery of the CCl_4. Measurements were made at room temperature with aqueous surfactant concentrations ranging from 0.1 to 7.5 mM. The interfacial tension was obtained from the drop volume by means of the method of Wilkinson.[51]

IV. Results

SF Vibrational Spectra. A representative sum-frequency vibrational spectrum of SDS adsorbed at the D_2O/CCl_4 interface at a 5.0 mM bulk concentration is displayed in Figure 2a. The spectrum was collected with p-polarized IR and visible light with no polarization selection for the generated sum-frequency light. This particular polarization combination results in a spectrum that displays contributions from both the in-plane and out-of-plane SF active vibrational modes. The vibrational spectra of DDS, DTAC, and DAC are similar to that of SDS with differences only in the relative peak intensities. Also shown is the nonresonant background from the D_2O/CCl_4 interface (Figure 2b). The spectrum in Figure 2a was fit with a combination of a Lorentzian and a Gaussian function for each peak. A Gaussian component was used in order to accommodate the limited bandwidth of the laser. No significant interference between the D_2O/CCl_4 nonresonant background and the resonant contribution for the adsorbed surfactant is apparent in the spectrum of SDS.

In order to make accurate spectral assignments, comparisons between the observed SF peaks and the corresponding infrared and Raman transition frequencies for poly(methylene) and long-chain alkanes have been made. The peak assignments for SDS,

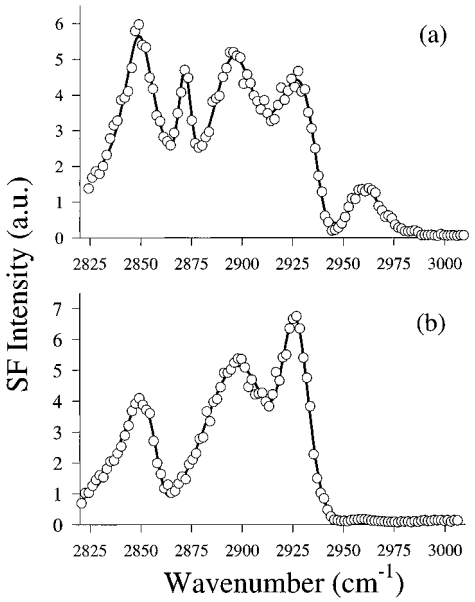

Figure 3. Sum-frequency vibrational spectrum of (a) hexadecyl sulfate, sodium salt, and (b) hexadecyl-d_3 sulfate, sodium salt. The spectra were obtained with p-polarized visible, p-polarized infrared, and no polarization selection of the output sum-frequency beam. Resonances at 2872 and 2960 cm^{-1} are assigned to the methyl symmetric and asymmetric stretch modes, respectively. The solid lines represent a fit to the spectra using a recombination of Gaussian and Lorentzian functions for each peak.

TABLE 1: SFG Peak Frequencies (cm^{-1}) of SDS, DDS, DTAC, and DAC Adsorbed at the D_2O/CCl_4 Interface and the Measured Infrared and Raman Band Frequencies (cm^{-1}) for Alkyl Chains

SFG		infrared		Raman	
2848	CH_2SS	2850	$d^+(\pi)$	2850	$d^+(0)$
2872	CH_3SS	2873	r^+	2871	r^+
2896	CH_2FR	2890	$d^+(\pi)_{FR}$	2898−2904	$d^+(0)_{FR}$
				2890	$d^-(0)$
2925	CH_2AS	2928	$d^-(\pi)$	2920−2930	$d^+(0)_{FR}$
2960	CH_3AS	2953−2962	r^-	2952−2964	r^-

DDS, DTAC, and DAC are summarized in Table 1. Also shown are the corresponding infrared and Raman modes and their respective frequencies.[52−57] Spectral assignments for the SF spectra of SDS shown in Figure 2a have been made as follows. The peaks at 2872 and 2960 cm^{-1} have been assigned to the terminal methyl symmetric (r^+) and asymmetric stretch (r^-) modes respectively. The peak at 2848 cm^{-1} has been assigned to the methylene symmetric resonance (d^+) of the hydrocarbon chain. The assignment of the peaks at 2896 and 2925 cm^{-1} are complicated by a difference between the IR and Raman data; see Table 1. The peak centered at 2896 cm^{-1} has been assigned to the symmetric methylene Fermi resonance (d^+_{FR}) resulting from interaction of an overtone of the methylene bending mode with the methylene symmetric stretch. This peak appears in the IR ($d^+(\pi)_{FR}$) at 2898−2904 cm^{-1} and in the Raman ($d^+(0)_{FR}$) at 2890 cm^{-1} of poly(methylene).[54,55] We have assigned the peak at 2925 cm^{-1} to the methylene asymmetric stretch (d^-) in agreement with the value observed in the IR spectrum (2920 cm^{-1}).[52] Previous SFG studies have assigned the peak between 2930 and 2940 cm^{-1} to the methyl symmetric stretch Fermi resonance peak (r^+_{FR}) and not the d^- mode.[29,30,39,58−60]

The above assignments have been verified by deuteration studies. Figure 3 displays the SF spectra of sodium hexadecyl sulfate (SHDS) (Figure 3a) and sodium hexadecyl-d_3 sulfate (Figure 3b), in which the terminal methyl group has been deuterated. The disappearance of the methyl peaks at 2872 and 2960 cm^{-1} for the r^+ and r^- modes respectively is seen upon deuteration. Comparison of the two spectra in Figure 3 also show that no detectable peak arising from the methyl Fermi resonance r^+_{FR} is observed in agreement with the assignment for the peak at 2925 cm^{-1} as the methylene asymmetric stretch and not the r^+_{FR} mode as reported by previous authors.[29,30,39,58−60] The peak at 2925 cm^{-1} remains strong in the spectrum of the deutered species, further verifying that this peak arises from the asymmetric methylene (d^-) mode. This assignment is in contrast to SFG spectra of surfactants adsorbed at the air/liquid interface where the methyl Fermi resonance at 2935 cm^{-1} is more pronounced.[61] The r^+_{FR} mode is also observed from self-assembled monolayers on metal substrates[39] and Langmuir-Blodgett films of cadmium arachidate on fused silica.[29,62] It is possible that in the spectra presented in this study that the methyl Fermi resonance is buried within the much stronger methylene mode.

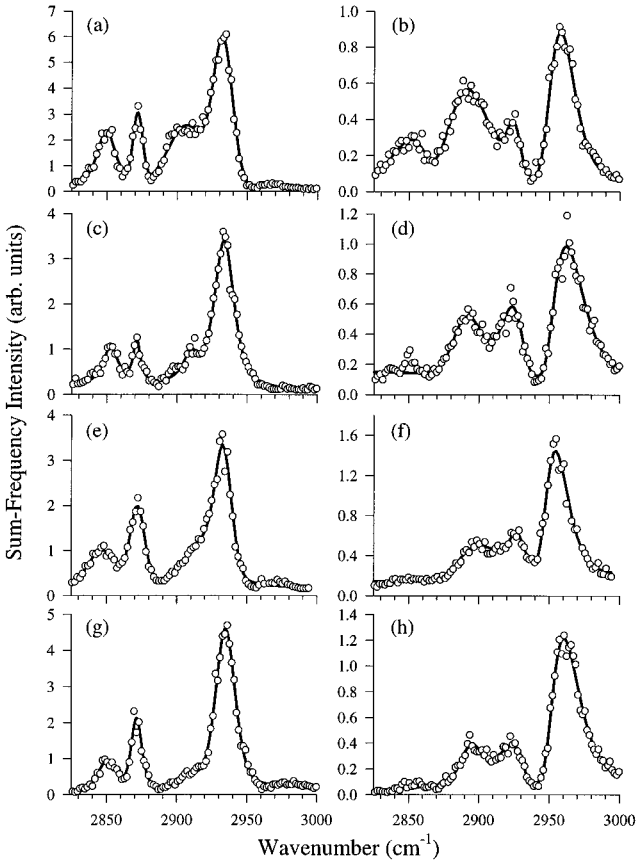

Figure 4. Sum-frequency vibrational spectra acquired with p-polarized infrared and s-polarized visible: (a) SDS, (c) DDS, (e) DTAC, and (g) DAC. SF spectra acquired with s-polarized infrared and p-polarized visible: (b) SDS, (d) DDS, (f) DTAC, and (h) DAC. Spectra were obtained at a bulk concentration of 5.0 mM. The generated sum-frequency was s-polarized in all cases. The solid lines represent a fit to the spectra using a combination of Gaussian and Lorentzian functions for each peak.

Figure 4 shows the SF spectra taken for SDS (4a,b), DDS (4c,d), DTAC (4e,f), and DAC (4g,h) at bulk concentrations of 5.0 mM. The first figure for each set represents the polarization combination of ssp (s-polarized SF, s-polarized visible, p-polarized IR) and the adjacent spectra were obtained with the polarization combination sps (s-polarized SF, p-polarized visible, s-polarized IR). The former polarization probes the out-of-plane components, whereas the latter, sps, polarization combination probes the in-plane components of the vibrational resonances. All spectra have been corrected for Fresnel factors so that the

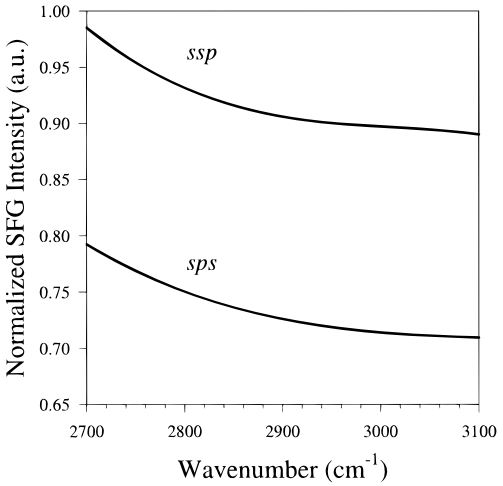

Figure 5. Calculated SF intensity as a function of IR and visible polarization for ssp and sps polarizations for the frequency range of 2700−3100 cm^{-1}.

intensities between the two polarizations can be compared quantitatively.

The SF spectra have been corrected for polarization and dispersion effects in the following way. There is a slight variation in the sum-frequency intensity as a function of the IR wavelength and polarization of the incident field independent of resonance effects. This variation is due to the change in the optical constants of the D_2O and CCl_4 within the spectral region of interest. By calculating the SF intensity for a specific experimental geometry and polarization of the input and output fields, the spectra can be normalized over the frequency region of interest. The real and imaginary components of the refractive index of D_2O[63] are used in conjunction with eqs 5a and 5b to calculate the SF intensity as a function IR wavelength for ssp and sps polarizations. The IR and visible fields are not significantly attenuated by the surface layer, as determined by reflection measurements. As a result, the refractive indices of the bulk phases are used in the determination of the nonlinear Fresnel coefficients as well.[36] The resulting SF intensity for the two polarization combinations as a function of IR frequency which were used to normalization the SF spectra in Figure 4 are shown in Figure 5.

The spectra taken using *p* polarized IR for all the surfactants studied (Figure 4a,c,e,g) exhibit strong intensities for the methylene asymmetric stretch (d^-), with peaks of moderate intensity observed for the methylene symmetric (d^+) and methyl symmetric (r^+) stretches. A weak methylene Fermi resonance (d^+_{FR}) is also observed as a shoulder of the methylene asymmetric stretch. For s polarization the asymmetric methylene (d^-) and methylene Fermi resonance (d^+_{FR}) are present in all cases. The most prominent feature in the *s*-polarized spectra of Figure 4b,d,f,h is the methyl asymmetric stretch (r^-) at 2960 cm^{-1}. A weak methylene symmetric stretch is also apparent.

SF spectra of SDS, DDS, DTAC, and DAC were collected at a number of aqueous surfactant concentrations ranging from 0.1 to 5.0 mM in D_2O. The symmetric methyl and methylene region of the vibrational spectra of SDS, DDS, DTAC, and DAC for 0.1 and 5.0 mM aqueous solutions are shown for ssp polarization in Figure 6. Strong C−H resonances are observed for both the d^+ and r^+ stretches. The spectra in Figure 6 have been normalized to the d^+ mode at 2850 cm^{-1} in order to compare relative intensities between spectra. A relative increase in the methyl symmetric stretch is observed between 0.1 and 5.0 mM bulk concentrations. The largest increase in the methyl

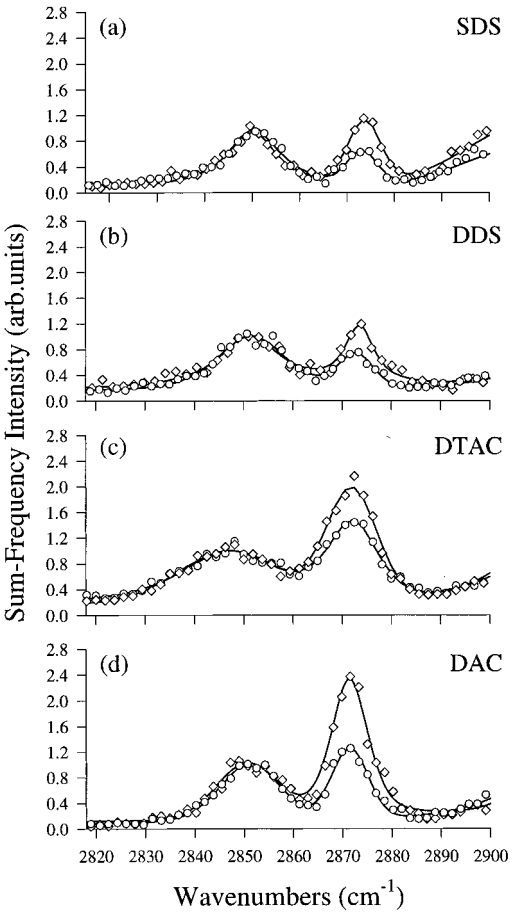

Figure 6. Sum-frequency vibrational spectra of the symmetric stretch region for (a) SDS, (b) DDS, (c) DTAC, and (d) DAC at the D_2O/CCl_4 interface. Spectra are shown for 0.1 mM (○) and 5.0 mM (◇) aqueous concentrations. The spectra were taken using s-polarized output, s-polarized visible, and p-polarized infrared. The solid lines represent a fit to the spectra using a combination of Gaussian and Lorentzian functions for each peak.

peak intensity is seen for DTAC and DAC. Even at the lowest concentration of 0.1 mM both DTAC and DAC possess the largest relative r^+ intensity compared to SDS and DDS at a bulk concentration of 5.0 mM.

In addition to the SF spectra, the interfacial pressure isotherms for SDS, DDS, DTAC, and DAC were also measured and are plotted in Figure 7. Measurements were taken between 0.1 and 7.5 mM bulk aqueous concentrations. All measurements were performed below the bulk critical micelle concentration of the surfactants. At a bulk concentration of 7.5 mM the surface pressures of SDS and DDS are the highest at 34 and 31 mN/m respectively. The cationic surfactants DTAC and DAC in comparison achieve a surface pressure of 24 and 28 mN/m respectively.

V. Discussion

Terminal Methyl Orientation. A determination of the average orientation of the terminal methyl group can be obtained from the polarization measurements presented in Figure 4. Components of transitions moments both parallel and perpendicular to the surface normal can be probed selectivity by using either p- or s-polarized IR respectively. Examination of the relative SF spectral intensities from both polarizations can in principle be used to determine the orientation of the hydrocarbon tail of the surfactant. In particular, the intensities of the methyl vibrational modes (r^+ and r^-) can be used to determine the average tilt angle of the terminal methyl with respect to the

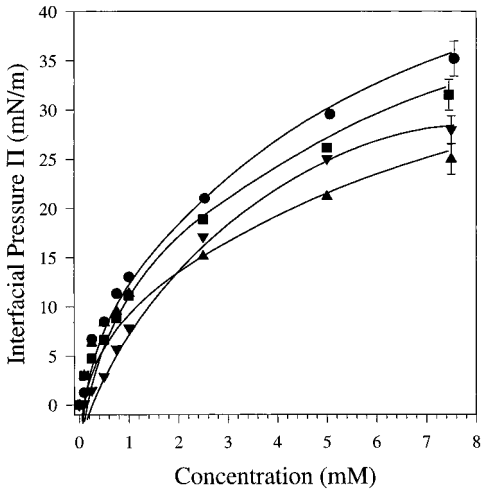

Figure 7. Plot of the interfacial pressure of (●) SDS, (■) DDS, (▲) DTAC, and (▼) DAC at the H_2O/CCl_4 interface versus the aqueous concentration. Measurements were obtained using the drop-volume method. Interfacial pressures were calculated by subtracting the value of the interfacial tension of the neat D_2O/CCl_4 interface. The solid line is shown as a guide to the eye.

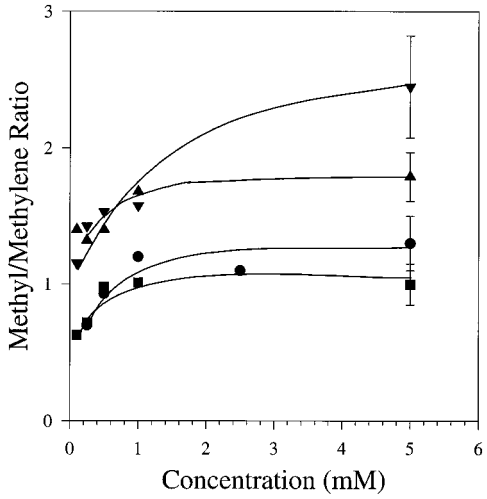

Figure 8. Plot of the ratio of the methyl symmetric stretch peak intensity (I_{r^+}) to the methylene symmetric stretch peak intensity (I_{d^+}) versus bulk aqueous concentration for (●) SDS, (■) DDS, (▲) DTAC, and (▼) DAC.

surface normal.[24,30,32,40,64] For a completely all-*trans* chain, the terminal methyl would be at an angle $\theta = 35°$ from the chain axis. For a monolayer that possesses symmetry in the plane of the surface, such as for a Langmuir−Blodgett film, components of both the r^+ and r^- modes should be observed under both p and s polarizations.[30,40,64] The spectra in Figure 4 for ssp polarization (p-polarized IR) show a pronounced CH_3 symmetric stretch at 2872 cm^{-1} (r^+) for all the surfactants examined. For the sps polarization (s-polarized IR) the symmetric stretch of the terminal methyl is not apparent. The absence of intensity with this polarization combination shows that no net polarization is induced in the plane of the surface for the r^+ mode. This suggests that the average orientation of the terminal methyl group for the ensemble is pointing primarily along the surface normal. This result is consistent with an isotropic distribution of molecules about the surface normal that would be expected at a liquid surface. The in-plane components of the r^+ mode effectively cancel for such an ensemble.

For the terminal methyl group, which possesses C_{3v} symmetry, the transition dipoles of the symmetric and asymmetric stretches are orthogonal to each other. Thus, the corresponding r^- mode can similarly be used in the determination of the orientation of the terminal methyl. For ssp polarization spectra shown in Figure 4a,c,e,g, negligible intensity of the r^- mode at 2960 cm^{-1} is observed. In contrast, when the IR light is polarized parallel to the surface, sps (Figure 4b,d,f,h) the most prominent feature in the spectra is the r^- mode at 2960 cm^{-1}. As with the symmetric CH_3 mode these results indicate that the average ensemble orientation of the terminal methyl is parallel to the surface normal. These results are found for the entire concentration range of SDS, DDS, DTAC, and DAC examined (0.1−5 mM) for both the r^+ and r^- modes. Conclusions regarding the absolute orientation or distribution of the alkyl chains are complicated by the fact that there appears to be a large number of gauche defects in the alkyl chains as evidenced by the strong symmetric methylene peak at 2850 cm^{-1} in the spectra of Figure 4a,c,e,g.

Conformation of the Alkyl Chain. To understand the relative intensities of the peaks in the SF spectra shown, it is necessary to consider the local symmetry of the CH_2 hydrocarbon backbone. An all-*trans* hydrocarbon chain is locally centrosymmetric with respect to methylene groups. Therefore, under the dipole approximation for SFG, little contribution from methylene resonances should be observed for a system of well-ordered (all-*trans*) hydrocarbon chains.[23,57] Because of this, the methyl and methylene region of the infrared spectrum is an especially sensitive indicator of conformation within the surfactant alkyl chain. The presence of a strong methylene peak necessarily leads to the conclusion that a number of gauche defects exist in the chain. The introduction of gauche conformations breaks the local symmetry of the hydrocarbon backbone, resulting in the previously forbidden methylene transitions to become allowed. The strong methylene peak in the spectra of Figure 4 indicates that all four surfactants studied have a considerable number of gauche defects within the alkyl chains and do not attain a well-ordered, all-*trans* configuration at the D_2O/CCl_4 interface at any surface coverages examined. This result is in contrast to surfactant adsorption at the solid/liquid or liquid/air interface in which an all-*trans* close-packed configuration of the alkyl chains can result.[23,40,65] Unlike amphiphiles adsorbed at the liquid/air interface, which exhibit significant ordering due to chain−chain van der Waals interactions, such chain interactions are reduced for amphiphiles at a nonpolar oil/water interface.[21,22,66] Chemisorption of the adsorbate head group onto a solid substrate, which often plays a role in molecular ordering at a solid/air interface, cannot occur at a liquid/liquid interface. The lack of head group localization and the inability to form strong chain−chain interactions contribute to the relative disorder of the hydrocarbon chain of surfactants at the liquid/liquid interface as compared to other interfaces.

To understand how the conformational order of the alkyl chains varies with surfactant concentration, the ratio of the intensities of the symmetric methyl and symmetric methylene stretch modes is compared. Previous studies have demonstrated that the I_{r^+}/I_{d^+} ratio can be used as an indictor of the relative order within the hydrocarbon chains.[67,68] The ratio of the methyl to methylene peak intensity, for the range of concentrations examined for SDS, DDS, DTAC, and DAC, are plotted in Figure 8. An increase in the I_{r^+}/I_{d^+} ratio is observed with increasing concentration, suggesting a change in the conformation of the alkyl chain with concentration. A decrease in the CH_2 symmetric stretch intensity for p-polarized IR indicates that the alkyl chains assume a conformation that contains fewer gauche defects, not simply a change in tilt angle or orientation along the surface normal. Although a change in the orientation of the hydrocarbon chain may be manifested as a reduction in the

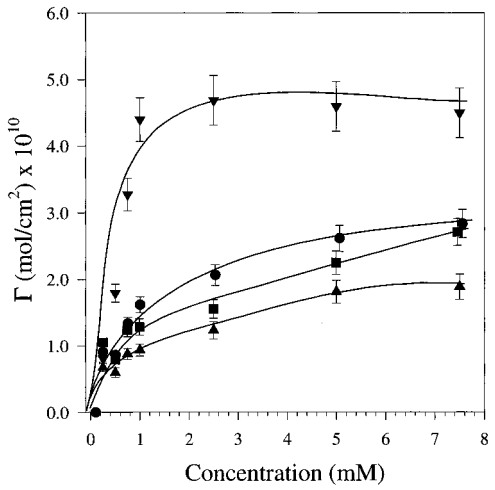

Figure 9. Surface excess concentration as a function of bulk aqueous concentration for (●) SDS, (■) DDS, (▲) DTAC, and (▼) DAC.

symmetric methyl stretch, the intensity of the symmetric methylene is dominated by the local break in symmetry of the hydrocarbons backbone and not the chain orientation. From the data in Figure 8 it appears that the ionic head group can play a role in the conformational behavior of these surfactants. The cationic surfactants, DTAC and DAC, possess the largest I_{r^+}/I_{d^+} ratio even at the lowest bulk concentrations. In contrast SDS and DDS show much smaller increases in the I_{r^+}/I_{d^+} ratio and show nearly identical behavior.

The effect of surface concentration on the conformational order within the alkyl chains determined from SF measurements is addressed. The surface excess concentration (Γ_i) of surfactant at the interface is obtained from the bulk aqueous concentration by way of the interfacial pressure isotherms. The interfacial tension curves for SDS, DDS, DTAC, and DAC at the D_2O/CCl_4 interface are shown in Figure 7. For highly surface active species such as these, the surface excess concentration can be considered to be equal to the actual surface concentration if adsorption of counterions does not compete significantly. The Gibbs equation used for calculating the surface excess as a function of bulk concentration in the absence of any supporting electrolyte is given by eq 6

$$\Gamma_i = \frac{1}{2RT}\left[\frac{\partial \pi}{\partial \ln(a_i)}\right]_T \qquad (6)$$

where π is the interfacial pressure in mN/m and a is the activity. For dilute solutions (less than 10^{-2} M), the activity can be replaced with the bulk concentration C_i. The surface concentrations of SDS, DDS, DTAC, and DAC obtained from eq 6 and the interfacial tension data are plotted in Figure 9.

The surface concentration as a function of bulk aqueous concentration plotted in Figure 9 shows a striking similarity to the I_{r^+}/I_{d^+} ratio data in Figure 8. This is consistent with the argument that as the surface density increases the degree of conformational mobility within the alkyl chains decreases, leading to more alkyl chain ordering. The cationic surfactant DAC that possesses the highest surface concentration also achieves the greatest I_{r^+}/I_{d^+} ratio in comparison to SDS, DDS, and DTAC. This trend can also be observed in the mean molecular areas at monolayer saturation for SDS, DDS, DTAC, and DAC. The cationic surfactant DAC possesses the smallest mean molecular area at 38 Å^2, whereas DTAC has a saturation area of 88 Å^2. SDS and DDS have areas of 59 and 61 Å^2 respectively. The surfactants SDS and DDS show very similar surface concentrations, which is also mirrored in the I_{r^+}/I_{d^+} values as observed in Figure 8. The I_{r^+}/I_{d^+} ratios obtained for SDS and DDS are consistently lower then those observed for DAC. Again this trend can be compared with their much lower surface concentrations and correspondingly higher molecular areas at monolayer saturation. However there is a clear discrepancy between the surface concentration data of DTAC and the I_{r^+}/I_{d^+} values seen in Figure 7. Although DTAC achieves lower surface coverages than SDS and DDS and possesses a much larger molecular area, the I_{r^+}/I_{d^+} ratios observed are larger than the anionic surfactants and more characteristic of those observed for DAC.

One explanation for this observation may be the solvation of the ionic head group. Solvation of the head group has two effects on the adsorbed surfactant molecules; one is the penetration depth of the ionic head group into the aqueous phase, and the other is surface roughness. Such microscopic parameters as the penetration depth and interfacial roughness of the adsorbed monolayer cannot be determined from the thermodynamic methods typically used to obtain macroscopic information about adsorbed films or by the spectroscopic methods employed here. Potentially, neutron reflection and X-ray scattering experiments might be able to provide the necessary microscopic and dynamic detail. However, at present these studies are limited in their usefulness in the investigation of liquid/liquid interfaces.[13,17,18] Although direct comparison between studies performed on the air/water and liquid/liquid interfaces is not necessarily accurate, such comparisons do lend some insight. For example, neutron reflection studies have found a difference in the penetration depth of the ionic head groups of SDS and hexadecyltrimethylammonium bromide (HDTAB) at the air/water interface.[14] The measured separation between the position of the ionic head group and that of the mean position of the aqueous interface is 7.5 ± 0.1 Å for SDS and 8.0 ± 0.1 Å for HDTAB.

If a similar increase in the penetration depth of the head group for DTAC and DAC as compared to SDS and DDS is occurring here, this may account for our spectroscopic observations. By drawing the alkyl chain further into the aqueous phase, the conformational fluidity of the alkyl chain can be reduced. Recent neutron reflection studies of dodecyltrimethylammonium bromide layers at the air/water interface have found that the majority of conformational defects in the hydrocarbon tail resides within the portion of the hydrocarbon chain furthest from the ionic head group.[16] The tilt angle of the portion of the alkyl chain closest to the head group is found to be nearly parallel with the surface normal, suggesting that the number of gauche defects within this portion of the chain are minimal. By drawing the head group further into the aqueous phase, the effective chain length in the organic phase is reduced, possibly making it more difficult for gauche defects to be introduced. This may account for the SF results that show that the alkyl chains of DTAC and DAC are found to possess fewer gauche defects than those of SDS and DDS.

In trying to understand the observed differences between the cationic and anionic surfactants presented above, possible effects due to contamination and interfacial pH should also be considered. Previous surface tension measurements of nonadodecylamine hydrochloride at the air/water interface have found that contaminants by carbonate ions greatly affects the surface activity.[69] In the experiments presented here no additional salts were added to the aqueous phase. The only possible contamination of carbonate ions would result from exposure to atmospheric CO_2. As was stated earlier, the experiments were conducted with a bulk pH ranging from 4.5 to 5. Since the pK_a values of carbonic acid are 6.37 and 10.25,[70] very little

free carbonate species should be present in our solutions. Another concern might be the effect of the surface pH resulting in an ill-defined protonation state of the surfactants, which might lead to ambiguities regarding the surface concentration due to the functional form of eq 6. This is particularly true for DAC, which has a bulk pK_a of 10.6.[71] The adsorption of a charged species on an interface alters the pH of the interface due to the potential difference arising from the adsorbed species.[66] In the case of the dodecylammonium ion the pK_a of an adsorbed monolayer is found to be somewhere between 8.5 and 10.0.[71] This is also substantiated by surface potential measurements of nonadodecylammonium chloride, which show no change below a bulk pH of 7.[69] This suggests that, at a bulk pH between 4.5 and 5 at which these SF experiments were performed, DAC is predominately in its protonated state. The fact that DAC is in a protonated state is consistent with the similarity between the SF results from DTAC and DAC, which show similar behavior as a function of surface concentration. Since DTAC is insensitive to pH, this suggests that the adsorbed DAC is in its protonated state.

Another plausible explanation for the discrepancy observed between the cationic and anionic surfactants could reside in the SF response for the bare D_2O/CCl_4 interface. Spectral interference between the nonresonant and resonant components of the induced sum-frequency response maybe contributing to the observed disparity. As was stated earlier the nonresonant background from the D_2O/CCl_4 interface was not measurable. However, even if a nondetectable intensity was arising from the interface, this may be sufficient to affect spectral features. Studies in this laboratory and others[61,72,73] of surfactants adsorbed at the air/H_2O and air/D_2O interfaces suggest that not only do the spectral features of H_2O and D_2O affect the intensities of the C−H region but also the relative intensity of the various resonances are dependent upon the ionic character of the head group, i.e. negative or positive charges. Such effects may be a factor in the observations made here. However, this is difficult to verify since a measurable background SF signal from D_2O is not observed in the studies presented here.

Mixed Ionic Surfactants. To further investigate the importance of the head group repulsion in alkyl chain ordering, the SFG spectra of a mixed anionic and cationic surfactant layer are examined. Although mixed anionic and cationic surfactants are incompatible in solution, forming insoluble precipitates, at extremely low concentrations the two can coexist in solution allowing adsorption at an interface. The strong electrostatic interactions between oppositely charged head groups result in unique properties of aqueous mixtures of anionic and cationic surfactants. An example of their unique properties can be seen in the increased surface activity of such a mixture compared to that of the pure surfactants.[74,75] If electrostatic head group repulsion is indeed determining alkyl chain order, a dramatic change in the I_{r^+}/I_{d^+} ratio should be observed. The SFG spectra of a mixed surfactant solution containing 0.05 mM DDS and 0.05 mM DAC is shown in Figure 10. For comparison the spectra of DAC and DDS at 0.1 mM are also shown. All spectra are shown for the symmetric stretch region for ssp polarization. Upon introduction of the oppositely charged surfactant, a dramatic increase in the methyl peak at 2872 cm^{-1} is observed with an accompanying decrease in the CH_2 symmetric stretch at 2850 cm^{-1}. In forming a mixed surfactant monolayer, the force responsible for limiting the packing density of the film, namely the electrostatic repulsion of similarly charged head groups, is removed. The result is that an extremely close-packed ensemble is formed, and this is manifested in the relatively high I_{r^+}/I_{d^+} ratio. DDS and DAC at 0.1 mM bulk aqueous concentration have a methyl/methylene ratio of 1.3 and 0.8 respectively. However, the mixed surfactant film of the same cumulative bulk surfactant concentration has a ratio of 2.4. This is a striking example of the head group packing density and its effect on the alkyl chain conformation as seen by SFG.

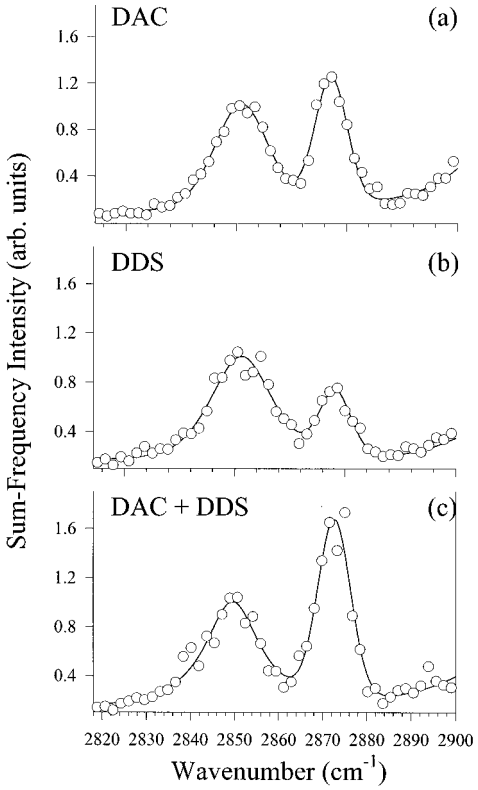

Figure 10. Sum-frequency vibrational spectra of the symmetric stretch region for (a) 0.1 mM DDS, (b) 0.1 mM DAC, and (c) 0.05 mM DDS + 0.05 mM DAC at the D_2O/CCl_4 interface. The spectra were taken using s/polarized output, s-polarized visible, and p-polarized infrared. The solid lines represent a fit to the spectra using a combination of Gaussian and Lorentzian functions for each peak.

IV. Conclusions

Sum-frequency vibrational spectroscopy has been used in this study to examine the molecular structure of four surfactants, SDS, DDS, DTAC, and DAC, adsorbed at the D_2O/CCl_4 interface. With the use of a TIR optical geometry, the sensitivity of this technique has been enhanced considerably allowing for the spectroscopic investigation of this previously inaccessible interface. The vibrational spectra reveal information on the orientation of the terminal methyl group as well as the conformation and order within the hydrophilic hydrocarbon chains. The surfactants studied all display identical C−H vibrational resonances. The C−H vibrational modes observed in the SF vibrational spectra were assigned and compared with the corresponding infrared and Raman transitions for similar compounds. These assignments were further verified with the use of a deuterated surfactant, hexadecyl-d_3 sulfate, in order to determine the contribution from the terminal methyl group to the SF spectra. In contrast to previous studies of water soluble surfactant at the air/water interface and amphiphiles adsorbed to solid substrates, the symmetric methyl Fermi resonance is not observed. Instead a pronounced asymmetric methylene resonance is found to be present.

Effects of the ionic head group on the conformation of the hydrocarbon chain and the orientation of the terminal methyl group have been studied. By examining the out-of-plane response of the SF vibrational spectra, the conformational

ordering of SDS, DDS, DTAC, and DAC was investigated. The CH_2 backbone displays pronounced resonances due to the symmetric and asymmetric methylene modes at 2850 and 2925 cm^{-1} respectively. The large intensity observed for these resonances is the result of the relaxation of the local symmetry constraint for the CH_2 vibrations by the introduction of gauche defects as the surface density increases. The ratio of the I_{r^+}/I_{d^+} methyl/methylene intensity as a function of bulk concentration is used as a measure of chain conformation. An increase in the I_{r^+}/I_{d^+} methyl/methylene ratio is observed with increasing surface coverage, suggesting a reduction in the number of gauche defects. The I_{r^+}/I_{d^+} ratio is seen to correlate well with the surface concentration obtained from interfacial tension measurements, demonstrating the effect of packing density on the ordering of the alkyl chains. From the spectral data DTAC and DAC are found to possess the least number of gauche defects relative to SDS and DDS at similar surface concentrations. For DTAC and DAC versus SDS and DDS, the greater penetration depth of the ionic head groups of DTAC and DAC into the aqueous phase may account for these observations.

Polarization studies were also performed in order to ascertain the orientation of the terminal methyl group of SDS, DDS, DTAC, and DAC at the D_2O/CCl_4 interface. The results indicate that the terminal methyl group is oriented primarily along the surface normal for all concentrations examined. This result is consistent with an isotropic distribution of molecules as would be expected for species adsorbed at the liquid/liquid interface. Any conclusions regarding the absolute orientation or orientation distribution of the alkyl chains, however, are complicated by the fact that there appears to be a large number of gauche defects in the alkyl chains as seen by the strong symmetric methylene resonance in the SF vibrational spectra.

Historically an investigation of molecular species adsorbed at a liquid/liquid phase boundary by conventional vibrational spectroscopy has been inaccessible. Complications arising from distinguishing between the spectral contributions of interfacial molecules and those in the more pervasive bulk have presented a formidable experimental challenge. These limitations have been overcome by the use of the surface selective technique of TIR SFG. The results reported here demonstrate the feasibility of the investigation of adsorption and transport properties at the interface between two immiscible liquids by nonlinear vibrational spectroscopy.

Acknowledgment. The authors gratefully acknowledge the skilled assistance of Dr. Jennifer Gage and the facilities provided by Professor Bruce Branchaud for the synthesis of hexadecyl-d_3 sulfate, sodium salt. In addition, the authors express appreciation to Ted Hinke for the construction of the cell. The starting material palmitic-d_3 acid was graciously provided by Professor Frederick Dahlquist. Funding is gratefully acknowledged from NSF (CHE 9416856) and the Petroleum Research Fund of the American Chemical Society.

References and Notes

(1) *Industrial Applications of Surfactants*; The Royal Society of Chemistry: Cambridge, U.K., 1992; Vol. 3.
(2) Myers, D. *Surface, Interfaces and Colloids: Principles and Applications*; VCH: New York, 1991.
(3) Myers, D. *Surfactant Science and Technology*; 2nd ed.; VCH Publishers, Inc.: New York, 1992.
(4) Wirth, M. J.; Burbage, J. D. *J. Phys. Chem.* **1992**, *96*, 9022.
(5) Piasecki, D. A.; Wirth, M. J. *J. Phys. Chem.* **1993**, *97*, 7700.
(6) Takenaka, T. T.; Nakanaga, T. *J. Phys. Chem.* **1976**, *80*, 475.
(7) Takenaka, T. *Chem. Phys. Lett.* **1978**, *55*, 515.
(8) Tian, Y.; Umemura, J.; Takenaka, T. *Langmuir* **1988**, *4*, 1064.
(9) Grubb, S. G.; Kim, M. W.; Rasing, T.; Shen, Y. R. *Langmuir* **1988**, *4*, 452.
(10) Higgins, D. A.; Corn, R. M. *J. Phys. Chem.* **1993**, *97*, 489.
(11) Higgins, D. A.; Naujok, R. R.; Corn, R. M. *Chem. Phys. Lett.* **1993**, *213*, 485.
(12) Bradley, J. E.; Lee, E. M.; Thomas, R. K.; Willatt, A. J.; Penfold, J.; Ward, R. C.; Gregory, D. P.; Waschkowski, W. *Langmuir* **1988**, *4*, 821−826.
(13) Lee, L. T.; Langevin, D.; Mann, E. K.; Farnoux, B. *Physica B* **1994**, *198*, 83.
(14) Lu, J. R.; Simister, E. A.; Lee, E. M.; Thomas, R. K.; Rennie, A. R.; Penfold, J. *Langmuir* **1992**, *8*, 1837−44.
(15) Lu, J. R.; Hromadova, M.; Simister, E. A.; Thomas, R. K.; Penfold, J. *J. Phys. Chem.* **1994**, *98*, 11519.
(16) Lyttle, D. J.; Lu, J. R.; Su, T. J.; Thomas, R. K.; Penfold, J. *Langmuir* **1995**, *11*, 1001−8.
(17) Lee, L. T.; Langevin, D.; Farnoux, B. *Phys. Rev. Lett.* **1991**, *67*, 2678−81.
(18) Cosgrove, T.; Eaglesham, A.; Horne, D.; Phipps, J. S. *Neutron Reflection from Liquid/Liquid Interfaces*; Springer-Verlag: Berlin, 1992; Vol. 61.
(19) Heinz, T. F.; Himpsel, F. J.; Palange, E.; Burstein, E. *Phys. Rev. Lett.* **1989**, *63* (6), 644−7.
(20) Roberts, G. *Langmuir-Blodgett Films*; Plenum Press: New York, 1990.
(21) Rosen, M. J. *Surfactants and Interfacial* Phenomena; John Wiley & Sons: New York, 1987.
(22) Tanford, C. *The Hydrophobic Effect: Formation of Micelles and Biological Membranes*; John Wiley & Sons: New York, 1973.
(23) Guyot-Sionnest, P.; Hunt, J. H.; Shen, Y. R. *Phys. Rev. Lett.* **1987**, *59* (14), 1597−1600.
(24) Hunt, J. H.; Guyot-Sionnest, P.; Shen, Y. R. *Chem. Phys. Lett.* **1987**, *133* (3), 189.
(25) Bain, C. D. *J. Chem. Soc., Faraday Trans.* **1995**, *91*, 1281.
(26) Miragliotta, J.; Polizzotti, R. S.; Rabinowitz, P.; Cameron, S. D.; Hall, R. B. *Chem. Phys.* **1990**, *143* (1), 123−30.
(27) Hall, R. B.; Russell, J. N.; Miragliotta, J.; Rabinowitz, P. R. *Springer Ser. Surf. Sci.* **1990**, *22* (Chem. Phys. Solid Surf. 8), 87−132.
(28) Hatch, S. R.; Polizzotti, R. S.; Dougal, S.; Rabinowitz, P. *J. Vac. Sci. Technol.* **1993**, *11* (4), 2232.
(29) Akamatsu, N.; Domen, K.; Hirose, C.; Onishi, T.; Shimizu, H.; Masutani, K. *Chem. Phys. Lett.* **1991**, *181* (2−3), 175−8.
(30) Hirose, C.; Yamamoto, H.; Akamatsu, N.; Domen, K. *J. Phys. Chem.* **1993**, *97*, 10064.
(31) Wolfrum, K.; Graener, H.; Laubereau, A. *Chem. Phys. Lett.* **1993**, *213*, 41−46.
(32) Wolfrum, K.; Lobau, J.; Laubereau, A. *Appl. Phys. A* **1994**, *59*, 605.
(33) Zhang, D.; Gutow, J.; Eisenthal, K. B. *J. Phys. Chem.* **1994**, *98*, 13729.
(34) Harris, A. L.; Rothberg, L.; Dhar, L.; Levinos, N. J.; Dubois, L. H. *J. chem. Phys.* **1991**, *94*, (4), 2438−48.
(35) Shen, Y. R. *The Principles of Nonlinear Optics*; Wiley: New York, 1984.
(36) Guyot-Sionnest, P.; Shen, Y. R.; Heinz, T. F. *Appl. Phys. B* **1987**, *42*, 237.
(37) Dick, B.; Gierulski, A.; Marowsky, G. *Appl. Phys. B* **1987**, *42*, 237.
(38) Shen, Y. R. *Nature (London)* **1989**, *337* (6207), 519−25.
(39) Bain, C. D.; Davies, P. B.; Ong, T. H.; Ward, R. N.; Brown, M. A. *Langmuir* **1991**, *7*, (8), 1563−6.
(40) Hirose, C.; Akamatsu, N.; Domen, K. *Appl. Spectrosc.* **1992**, *46*, 1051.
(41) Hunt, J. H.; Guyot-Sionnest, P.; Shen, Y. R. *Chem. Phys. Lett.* **1987**, *133*, 189.
(42) Haller, G. L.; Rice, R. W. *J. Phys. Chem.* **1970**, *74*, 4386.
(43) Harrick, N. J.; du Pre, F. K. *Appl. Opt.* **1966**, *5*, 1739.
(44) Harrick, N. J. *Internal Reflection Spectroscopy*; Wiley-Interscience: New York, 1967.
(45) Bloembergen, N.; Pershan, P. S. *Phys. Rev.* **1962**, *128*, 606.
(46) Bloembergen, N. *Opt. Acta* **1966**, *13*, 311.
(47) Bloembergen, N.; Simmon, H. J. *Phys. Rev.* **1969**, *181*, 1261.
(48) Fieser, L. F.; Fieser, M. *Reagents for Organic Synthesis*; Wiley: New York, 1967.
(49) Wong, E. K. L. *Comparative Studies of Optical Second Harmonic Generation of Single Crystal Noble Metal Electrodes Under Resonant and Non resonant Conditions*; Wong, E. K. L., Ed.; University of Oregon: Eugene, OR, 1992; p 180.
(50) Adam, N. K. *The Physics and Chemistry of Surfaces*; 3rd ed.; Oxford University Press: London, 1941.
(51) Wilkinson, *J. Colloid Interface Sci.* **1972**, *40*, 14.
(52) Snyder, R. G.; Hsu, S. L.; Krimm, S. *Spectrochim. Acta* **1978**, *34A*, 395.
(53) Snyder, R. G.; Scherer, J. R. *J. Phys. Chem.* **1979**, *71*, 3221.
(54) Snyder, R. G.; Strauss, H. L.; Elliger, C. A. *J. Phys. Chem.* **1982**, *86*, 5145.

(55) MacPhail, R. A.; Strauss, H. L.; Snyder, R. G.; Elliger, C. A. *J. Phys. Chem.* **1984**, *88*, 334−41.
(56) Cates, D. A.; Strauss, H. L.; Snyder, R. G. *J. Phys. Chem.* **1994**, *98*.
(57) Aljibury, A. L.; Snyder, R. G.; Strauss, H. L.; Raghavachari, K. *J. Phys. Chem.* **1986**, *84*, 6873.
(58) Bain, C. D. *Langmuir* **1994**, *10*, 2060.
(59) Ward, R. N.; Duffy, D. C.; Davies, P. B.; Bain, C. D. *J. Phys. Chem.* **1994**, *98*, 8536.
(60) Guyot-Sionnest, P.; Superfine, R.; Hunt, J. H.; Shen, Y. R. *Chem. Phys. Lett.* **1988**, *144*, 1.
(61) Bell, G. R.; Bain, C. D.; Ward, R. N. *J. Chem. Soc., Faraday Trans.* **1995**, *92*, 515−23.
(62) Akamatsu, N.; Domen, K.; Hirose, C. *J. Phys. Chem.* **1993**, *97*, 10070.
(63) Bertie, J. E.; Ahmed, M. K.; Eysel, H. H. *J. Phys. Chem.* **1989**, *93*, 2210.
(64) Goto, Y.; Akamatsu, N.; Domen, K.; Hirose, C. *J. Phys. Chem.* **1995**, *99*, 4086.
(65) Golden, W. G.; Snyder, C. D.; Smith, B. *J. Phys. Chem.* **1982**, *86* (24), 4675.
(66) MacRitchie, F. *Chemistry at Interfaces*; Academic Press, Inc.: New York, 1990.
(67) Messmer, M. C.; Conboy, J. C.; Richmond, G. L. *J. Am. Chem. Soc.* **1995**, *117*, 8039.
(68) Conboy, J. C.; Messmer, M. C.; Richmond, G. L. *J. Phys. Chem.* **1995**, *100*, 7617−22.
(69) Betts, J. J.; Pethica, B. A. *Trans. Faraday Society* **1956**, *52*, 1581.
(70) *CRC Handbook of Chemistry and Physics*, 62nd ed.; CRC Press Inc.: Boca Raton, FL, 1981−1982.
(71) Tchaliovska, S.; Manev, E.; Radoev, B.; Eriksson, J. C.; Claesson, P. M. *J. Colloid Interface Sci.* **1994**, *168*, 190−97.
(72) Gragson, D. E.; McCarty, B. M.; Richmond, G. L. *J. Phys. Chem.* **1996**, *100*, 14272.
(73) Gragson, D. E.; McCarty, B. M.; Richmond, G. L. *J. Am. Chem. Soc.* in press.
(74) Kaler, E. W.; Herrington, K. L.; Miller, D. D.; Zasadzinski, J. A. N. *Phase Behavior of Aqueous Mixtures of Anionic and Cationic Surfactants Along a Dilution Path*; Kaler, E. W.; Herrington, K. L.; Miller, D. D.; Zasadzinski, J. A. N., Eds.; Kluwer Academic Publishers: Dorchester, 1992; pp 571−577.
(75) Lucassen-Reynders, E. H.; Lucassen, J.; Giles, D. *J. Colloid Interface Sci.* **1981**, *81*, 150.